Temperature-dependent photoluminescence of GaInP/AlGaInP multiple quantum well laser structure grown by metalorganic chemical vapor deposition with tertiarybutylarsine and tertiarybutylphosphine

C. Y. Liu and Shu Yuan[a)]
School of Materials Engineering, Nanyang Technological University, Singapore, 639798

J. R. Dong and S. J. Chua
Institute of Materials Research and Engineering, 3 Research Link, Singapore, 117602

M. C. Y. Chan
Department of Electrical and Electronic Engineering, University of Hong Kong, Hong Kong, People's Republic of China

S. Z. Wang
School of Electrical and Electronic Engineering, Nanyang Technological University, Singapore, 639798

(Received 26 March 2003; accepted 10 June 2003)

A GaInP/AlGaInP multiple quantum well laser structure was grown by low-pressure metalorganic chemical vapor deposition with tertiarybutylarsine and tertiarybutylphosphine. Laser diodes fabricated from this structure lased at room temperature. Photoluminescence (PL) measurements were performed from 10 to 230 K. The PL energy increased with temperature from 10 to 70 K and decreased above 70 K. The former was attributed to thermal activation of trapped carriers due to localization in the quantum wells, while the latter was attributed to temperature-induced band-gap shrinkage. The PL intensity as a function of temperature was fitted by employing two nonradiative recombination mechanisms with good agreement, resulting in two activation energies that correspond to losses of photogenerated carriers to nonradiative centers. © *2003 American Institute of Physics.* [DOI: 10.1063/1.1597977]

I. INTRODUCTION

GaInP/AlGa1nP laser diodes (LDs) grown on GaAs substrates by metalorganic chemical vapor deposition (MOCVD) have been intensively developed for 630–700 nm wavelength range applications, such as laser pointers, barcode readers, and digital versatile disk (DVD) players.[1–4]

In most cases, GaInP/AlGaInP laser structures are produced by employing MOCVD with hazardous group-V hydride gases, such as arsine (AsH_3) and phosine (PH_3). The hazards involved have been a major concern in the MOCVD process. Thus, less toxic organic group-V MOCVD sources, such as tertiarybutylarsine (TBAs) and tertiarybutylphosphine (TBP), have been used to replace group-V hydrides because of reduced hazards.[5–11] Devices grown with TBAs and TBP have exhibited state-of-the-art performances in InGaAsP lasers and GaInAs/GaAs/GaInP lasers.[7–9] However, there have been few reports on high-quality GaInP/AlGaInP quantum well (QW) structures grown by MOCVD with TBAs and TBP, which can be used for active layers of devices, such as light emitting diodes (LEDs) and LDs.[10,11] To date, only Itaya *et al.*[10] have reported low-temperature (77 K) pulsed operation of GaInP/AlGaInP lasers grown by MOCVD with TBAs and TBP. Their results show that, unlike conventional MOCVD growth with AsH_3 and PH_3, GaInP/AlGaInP lasers grown by MOCVD with TBAs and TBP have problems regarding generation of nonradiative recombination centers in the Al-containing cladding or barrier layers.[10] Furthermore, the threshold current density of GaInP/AlGaInP lasers grown with TBAs and TBP is very sensitive to the temperature, which is ascribed to higher nonradiative recombination rates at higher temperatures, since the nonradiative recombination centers could be activated by increasing temperature.[10] Such results indicate that the temperature-dependent behavior of carriers in MOCVD grown GaInP/AlGaInP QWs with TBAs and TBP is important for device applications. Therefore, a systematic investigation of the photoluminescence (PL) properties of this material system at different temperatures is necessary for understanding its light emission mechanisms. However, there has been no report on the temperature-dependent PL properties of GaInP/AlGaInP laser structures grown by MOCVD with TBAs and TBP.

In this work, a GaInP/AlGaInP multiple quantum well (MQW) laser structure was grown by low-pressure MOCVD (LP-MOCVD) with TBAs and TBP as group-V sources. Pulsed-mode operations at room temperature of ridge waveguide lasers fabricated from this material system has been realized.[12] Temperature-dependent PL measurements were performed in the temperature range from 10 to 230 K. A two nonradiative recombination mechanisms model was presented to interpret the PL emission behavior over the experimental temperature range.

[a)]Author to whom correspondence should be addressed; electronic mail: assyuan@ntu.edu.sg

TABLE I. Sample structure.

Layer	Thickness (nm)	Doping concentration (cm^{-3})
GaAs	150	Zn: 1×10^{19}
GaInP	100	Zn: 2×10^{18}
$(Al_{0.7}Ga_{0.3})_{0.52}In_{0.48}P$	1200	Zn: 1×10^{18}
$(Al_{0.7}Ga_{0.3})_{0.52}In_{0.48}P$	50	Undoped
$(Al_{0.4}Ga_{0.6})_{0.52}In_{0.48}P$	80	Undoped
$Ga_{0.49}In_{0.51}P/(Al_{0.4}Ga_{0.6})_{0.52}In_{0.48}P$	3 periods, 8/10	Undoped
$(Al_{0.4}Ga_{0.6})_{0.52}In_{0.48}P$	80	Undoped
$(Al_{0.7}Ga_{0.3})_{0.52}In_{0.48}P$	30	Undoped
$(Al_{0.7}Ga_{0.3})_{0.52}In_{0.48}P$	800	Si: 2×10^{18}
GaInP	60	Si: 2×10^{18}
GaAs	200	Si: 2×10^{18}
n^+-GaAs substrate (100), 7° off axis towards (111) *A*		

II. MATERIAL GROWTH AND EXPERIMENTAL PROCEDURE

The MQW laser structure is shown in Table I. The wafer was grown by a low-pressure horizontal MOCVD system with planetary rotation to ensure the uniformity of the grown epitaxial materials. AlGaInP epilayers were grown on n^+-GaAs (100) substrates 7° off towards (111) *A* to suppress the spontaneous ordering in the GaInP and AlGanP epilayers. Trimethylgallium (TMGa), trimethylindium (TMIn), and trimethylaluminum (TMAl) were used as group-III sources; tertiarybutylarsine and tertiarybutylphosphine were utilized as group-V sources. Silane (SiH_4) and diethylzinc (DEZn) were the *n*- and *p*-type doping sources, respectively. H_2 was used as carrier gas. The growth temperature was 675 °C measured by a thermocouple inserted in the graphite susceptor. The growth chamber pressure was set at 100 mbars. The V/III ratio was 75 and the growth rate was about 1 μm/h. The choice of V/III ratio was as following: GaInP was first grown lattice matched to GaAs substrate. AlGaInP was subsequently grown by introducing an Al source while Ga source flow rate was reduced correspondingly to keep the AlGaInP lattice matched to GaAs substrates. The optical quality of AlGaInP epilayers strongly depends on the V/III ratio as in the case of phosphine-based AlGaInP. The PL intensity increases dramatically with increasing V/III ratio, and saturates above 75. Therefore, afterwards all the AlGaInP layers were grown at V/III ratio of 75.

Ridge waveguide lasers were fabricated with a contact ridge width of 50 μm and isolated by pulsed anodic oxidation.[13] Details of the laser work will be published elsewhere.

The PL measurements were performed in the temperature range from 10 to 230 K using the 488 nm line of a 40 mW Ar^+ laser, a closed cycle cryostat, a 0.5 m spectrometer, a thermal electric cooled silicon detector, and a lock-in amplifier. Before the PL measurement, the top contact layer and most part of the top cladding layer were etched at 22 °C by $H_3PO_4:H_2O_2:5H_2O$ and $HCl:3H_3PO_4$, respectively, and the total etch depth was about 1 μm.

TABLE II. Material parameters of GaP, InP, and AlP used in the calculations (see Refs. 17 and 18).

	GaP	InP	AlP
E_g at 300 K	2.78 eV	1.34 eV	3.56 eV
E_g at 0 K	2.857 eV	1.411 eV	3.637 eV
m_c at 300 K	0.158 m_o	0.077 m_o	0.212 m_o
m_{hh} at 300 K	0.54 m_o	0.45 m_o	0.513 m_o
m_{lh} at 300 K	0.162 m_o	0.089 m_o	0.211 m_o
m_c at 77 K	0.17 m_o	0.08 m_o	0.212 m_o
m_{hh} at 77 K	0.67 m_o	0.56 m_o	0.513 m_o
m_{lh} at 77 K	0.17 m_o	0.12 m_o	0.211 m_o

III. MODELING OF INTERBAND TRANSITION ENERGIES AND PL INTENSITY

The knowledge of the interband transition energy is important in determining whether the observed PL is from the interband transition or from other radiative recombination channels. The subband energies E_r at the band edge of the QW were calculated by a Schrödinger-like equation using the envelope function approximation method as given below:[14]

$$-\frac{\hbar^2}{2}\frac{d}{dz}\left[\frac{1}{m_r^*}\frac{d\psi_r}{dz}\right]+U_r\psi_r=E_r\psi_r, \tag{1}$$

where the subscript r denotes either the electrons ($r=e$), heavy holes ($r=$hh), or light holes ($r=$lh). $\psi_r(z)$ denotes the wave function, U_r is the subband energy in the quantum well, and m_r^* is the corresponding carrier effective mass in the z direction. A conduction-band offset of 0.65 was used in the calculation.[15] The values for effective masses were determined by interpolations of the binary parameters by Vegard's Law. The parameters used in the calculation are listed in Table II. After the subband energy E_r was calculated, the interband transition energy was evaluated and compared to measured PL photon energy.

The temperature-dependent energy gap of a semiconductor alloy is given by Varshni relation:[16]

$$E_g(T)=E_g(T=0)-\frac{\alpha T^2}{T+\beta}, \tag{2}$$

where α and β are constants.

Temperature-dependent band gaps of binary alloys GaP, AlP, and InP were calculated following Eq. (2). We choose $\alpha=0.5771$ meV/K, $\beta=372$ K for both GaP and AlP, and $\alpha=0.363$ meV/K, $\beta=162$ K for InP.[17,18]

For the ternary semiconductor alloys GaInP and AlInP discussed here, the temperature dependence of the energy gap on alloy composition was assumed to fit a simple quadratic form:[17]

$$E_g(A_{1-x}B_xC)=(1-x)E_g(A)+xE_g(B)-x(1-x)P, \tag{3}$$

where the so-called bowing parameter P accounts for the deviation from a linear interpolation between the two binaries A and B. Here, we choose the bowing parameter $P=0.65$ eV for GaInP and $P=-0.48$ eV for AlInP, respectively.[17]

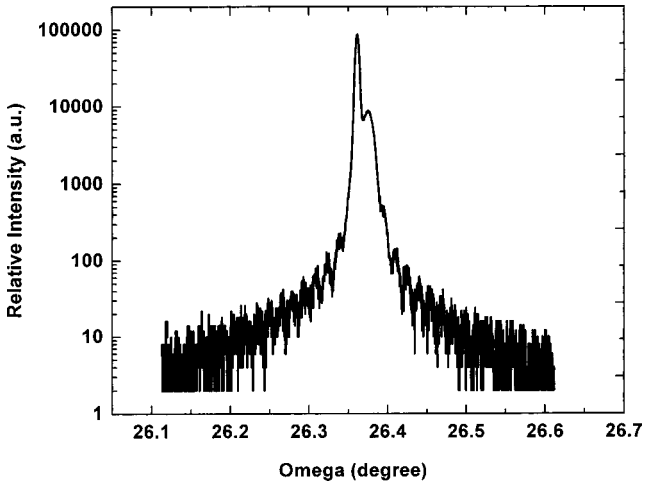

FIG. 1. X-ray diffraction spectrum of an $(Al_{0.7}Ga_{0.3})_xIn_{1-x}P$ epilayer reference sample.

Similarly, the temperature-dependent band-gap energy of the $(Al_{0.4}Ga_{0.6})_{0.52}In_{0.48}P$ barrier layer discussed here was determined by an interpolation of the ternary alloy of $Al_{0.52}In_{0.48}P$ and $Ga_{0.52}1In_{0.48}P$ with the bowing parameter P of 0.18 eV as shown below:[17]

$$E_g[(Al_xGa_{1-x})_{0.52}In_{0.48}P] = xE_g(Al_{0.52}In_{0.48}P) + (1-x)E_g(Ga_{0.52}In_{0.48}P) - x(1-x)P. \quad (4)$$

In this work, the integrated PL intensity as a function of inverse temperature was fitted with the following model involving two nonradiative recombination mechanisms described by[19–21]

$$I = I_0\ [1 + C_1 \exp(-E_1/k_BT) + C_2 \exp(-E_2/k_BT)]^{-1}, \quad (5)$$

where I is the integrated PL intensity; I_0 is the integrated PL intensity at the low temperature limit; C_1, C_2 are fitting constants; E_1 and E_2 are the activation energies at the two different temperature regions; k_B is the Boltzmann constant; and T is the sample temperature.

IV. RESULTS AND DISCUSSION

X-ray diffraction spectroscopy measurements were used to check the growth quality. Figure 1 shows a typical x-ray diffraction spectrum of an $(Al_{0.7}Ga_{0.3})_xIn_{1-x}P$ epilayer on a GaAs substrate. The Pendellösung fringes can be observed indicating the abrupt interface between AlGaInP and GaAs and uniform composition along the growth direction. By simulating the fringes based on dynamical theory, the $(Al_{0.7}Ga_{0.3})_xIn_{1-x}P$ thickness of 435 nm and In composition of 48.3% can be obtained.

Figure 2(a) shows a typical light output power versus current characteristics (L–I) of ridge waveguide lasers fabricated from the wafer. The ridge width was 50 μm and isolated by using pulsed anodic oxidation,[13] the cavity length was 1200 μm, and no facet coating was applied to the as-cleaved lasers. The lasers were tested under pulsed operation

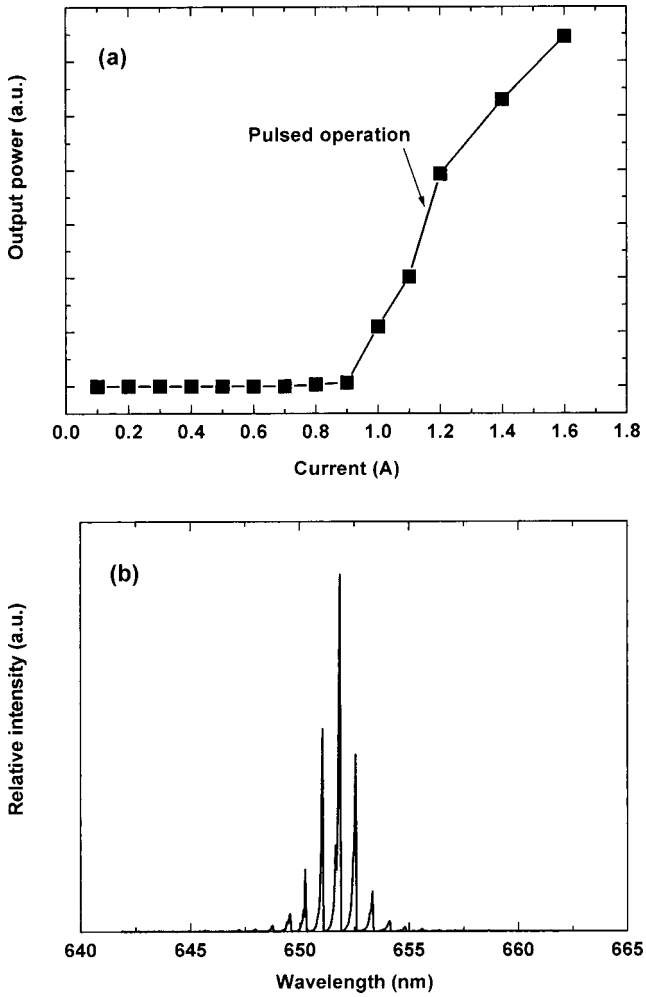

FIG. 2. (a) Room-temperature light output power vs injection current for a ridge waveguide GaInP/AlGaInP laser isolated by pulsed anodic oxidation. Ridge width=50 μm, cavity length=1200 μm, frequency=10 kHz, duty cycle=1%, and pulse width=1 μs. (b) Emission spectrum taken at $I = 1.1 \times I_{th}$ at room temperature.

without proper heatsink (frequency=10 kHz, duty cycle =1%, pulse width=1 μs). The threshold current density was 1.5 kA/cm^2. Broad area lasers were also fabricated by Dong *et al.*[12] from wafers grown together in the same batch and a threshold current density of 5 kA/cm^2 was obtained. Figure 2(b) shows the corresponding laser emission spectrum measured at an inject current of $1.1 \times I_{th}$. No room-temperature operation of GaInP/AlGaInP lasers fabricated from wafers grown by MOCVD using TBAs and TBP have been reported by other groups.

Figure 3 shows the PL spectra of the laser structure at 10, 100, and 230 K, respectively. The 10 K spectrum is dominated by a single narrow sharp emission peak at 1.995 eV with the full width at half maximum (FWHM) of 20.85 meV. The luminescence was observed up to about 230 K.

The interband transition energy as a function of temperature was calculated using the model described in Sec. III. The results (line) are compared to the PL peak position (dots) in Fig. 4. The calculated interband transition energy decreases monotonously due to band-gap shrinkage with temperature as expected from Eq. (2). However, in the low-

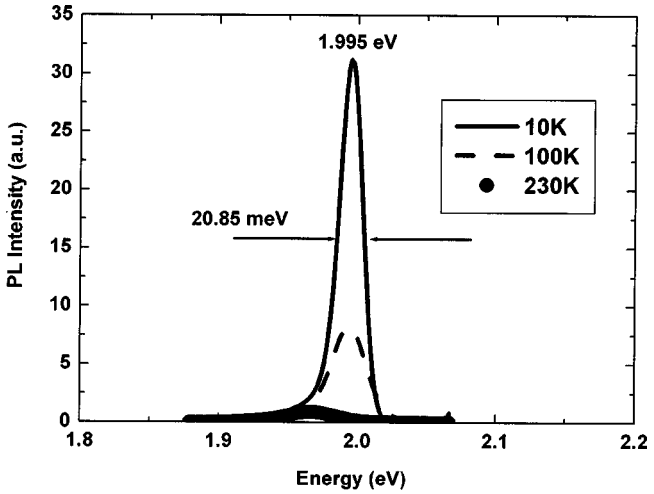

FIG. 3. PL spectra from the laser structure at 10, 100, and 230 K, respectively. The wafer was etched by 1 μm before the PL measurements, thus the top GaAs contact layer and most part of the top cladding layer were removed.

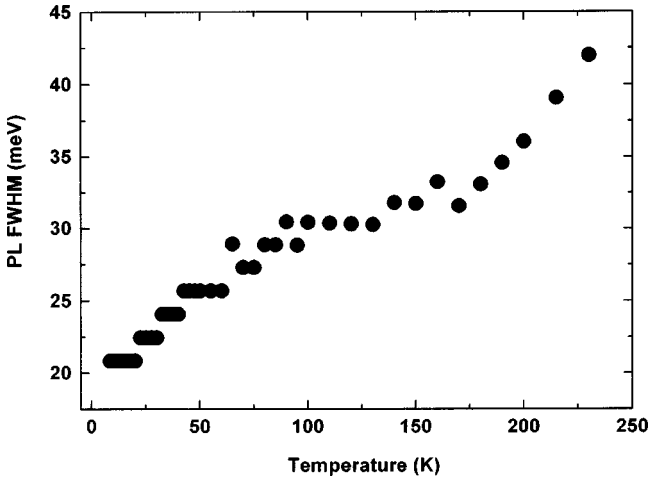

FIG. 5. PL linewidth (FWHM) of the laser structure as a function of temperature.

temperature region the PL peak position increases with temperature, reaching a maximum at 70 K. The blueshift from 10 to 70 K is 3 meV. In the higher-temperature region from 70 K above, the PL peak decreases with temperature, following the trend of the calculated interband transition energy. The blueshift phenomenon at the low-temperature region was also reported in bulk GaInP,[22] in InGaN,[23] and in GaAs quantum wells.[24,25] It is believed to be caused by the localization of the carriers at low temperatures. A combination of possible composition fluctuation and well width fluctuation and interface roughness of the QWs produces an effective band-gap modulation in the growth direction, and thus causes local potential fluctuations, giving rise to a statistical distribution of local potential minima. At low temperatures, the minima act as trap sites. Photogenerated carriers drift towards the potential minima as drift times are much shorter than radiative recombination times, the carriers are trapped by these potential fluctuations, i.e., a kind of localization.[25] In the low-temperature region, when temperature is increased, more carriers are thermally activated from localized regions and are able to occupy higher-energy states in the band-gap modulation scheme. Consequently, the QW peak should be broadened and shifted towards higher energies, i.e., blueshift. We concluded that the PL peak blueshift in our sample was due to thermally activated trapped carriers in localized regions, blueshifting the PL peak. As the temperature was further increased to above 70 K, most of the trapped carriers attained more thermal energy and were ''thermalized'' out from the local potentional traps. These free carriers recombined in the quantum well through the interband transition recombination process. The interband transition energy decreased monotonously, as the band gap decreased with temperature according to Eq. (2), i.e., when $T \geqslant 70$ K, the PL peak began to redshift.

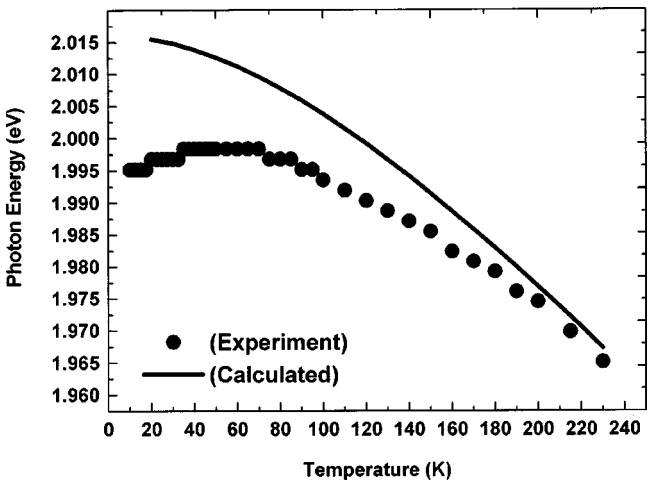

FIG. 4. Comparison between measured PL peak energy (dots) and calculated interband transition energy (line) as a function of temperature.

The temperature-dependent linewidth (FWHM) of the PL peak is shown in Fig. 5. The linewidth increased with temperature in the whole temperature range. For the interband transition, the linewidth should follow a liner temperature dependence[21] and this was observed in Fig. 5 for temperatures above $\sim$150 K. Below this temperature, the linewidth did not follow the same line, indicating the PL was not purely from interband transition in the quantum well. The temperature dependence of the linewidth below $\sim$70 K likely represented the radiative transitions by carriers that were trapped by the localization potential minima. The region between $\sim$70 and 150 K could be due to a transition from a radiative recombination of localized carriers to a radiative recombination of free carriers, i.e., the interband transition.

Figure 6 shows the integrated PL intensity as an inverse function of temperature. The dots are the experimental data. At low temperatures, the integrated PL intensity dropped slowly with temperature. At high temperatures, it decreased more rapidly with temperature. This behavior suggests the presence of two nonradiative recombination mechanisms, corresponding to two different activation energies at these different temperature regions. The PL intensity as a function of inverse of temperature was fitted by using the model outlined in Sec. III. The solid line shown in Fig. 6 is the best fit

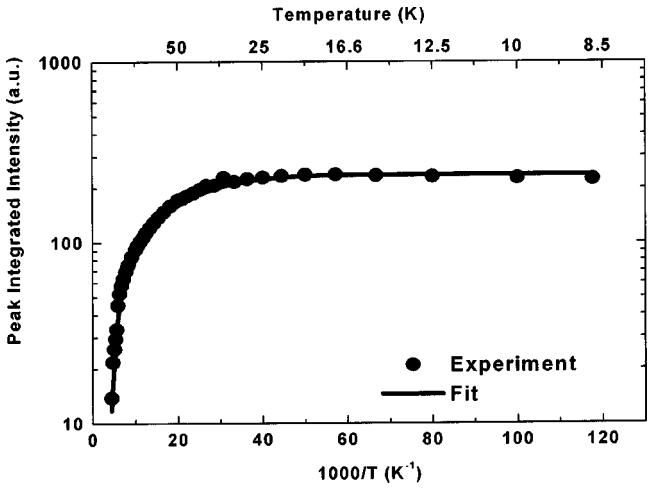

FIG. 6. Arrhenius plot of integrated PL intensity of emission peak as function of inverse temperature for the laser structure. Dots are the experimental data, and the solid line is the best fit using two nonradiative recombination mechanisms model, ($C_1=3.9$, $C_2=1565$, $E_1=9$ meV, $E_2=90$ meV).

for the entire temperature range, which yielded C_1 of 3.9 and C_2 of 1565 and activation energies E_1 of 9 meV and E_2 of 90 meV, respectively. C_1 and E_1 correspond to the low-temperature range; C_2 and E_2 correspond to the higher-temperature range. The temperature-dependent PL intensity could be explained as the following: since the top contact layer of the wafer and most part of the top cladding layer were etched before PL measurements, the excitation laser beam (wavelength$=488$ nm, photon energy~ 2.54 eV) was absorbed in the remaining top cladding layer [p-type $(Al_{0.4}Ga_{0.6})_{0.52}In_{0.48}P$, about 450 nm left after wet etching] and the $(Al_{0.4}Ga_{0.6})_{0.52}In_{0.48}P$ barrier layers and the $Ga_{0.49}In_{0.51}P$ quantum wells, thus photogenerated carriers originate from these layers will all contribute to the carrier recombination in the GaInP quantum well. At low temperatures, the photogenerated carriers were captured by the localized potential minima that acted as active radiative recombination centers, but some of the photogenerated carriers were lost to nonradiative recombination centers, reducing the PL intensity. This mechanism had an activation energy $E_1=9$ meV. At high temperatures, however, another type of nonradiative recombination centers was thermally activated, which trapped photogenerated carriers before they recombined radiatively, thus reducing the PL intensity significantly. Similar behavior of temperature-dependent PL intensity was observed in GaInP/AlGaInP quantum wells by Michler *et al.*[21] who reported that the activation energy E_2 is equal to one half of the total confinement energy ΔE_{TOL} of the electron–hole pair in the quantum well. They concluded that carriers were lost from the quantum well to the barrier layers. In our work the total confinement energy ΔE_{TOL} can be calculated as $\Delta E_{\mathrm{TOL}}=$energy gap of the barrier-PL energy. $\Delta E_{\mathrm{TOL}}/2$ was found to be ~ 111 meV, insensitive to temperature variations. This is larger than the activation energy E_2 (90 meV) determined by fitting to data in Fig. 6. The photogenerated carriers were likely lost to the barriers, where they were possibly captured by nonradiative centers. The nature of the nonradiative centers is not clear from this work; we suspect they originated from defects and impurities in the AlGaInP barrier layer during the growth. More work on defects and impurities on AlGaInP grown by MOCVD with TBP and TBAs is needed to yield more information on the nature of the nonradiative centers.

V. CONCLUSIONS

In summary, a GaInP/AlGaInP quantum well laser structure was grown by LP-MOCVD using TBAs and TBP. X-ray diffraction was used to check the quality of the growth. Laser diodes were fabricated from this material system by using a pulsed anodic oxidation method. The laser diodes worked under pulsed operation at room temperature. Temperature-dependent PL measurements from the laser structures were carried out systematically from 10 to 230 K. The interband transition energy was calculated by using the envelope function approximation method. Blueshift of PL energy with increasing temperature from 10 to 70 K was observed and was interpreted based on thermalization of localized carriers. A model of two nonradiative recombination mechanisms was used to fit the temperature-dependent PL intensity with good agreement with the experimental data.

ACKNOWLEDGMENTS

The authors thank Dr. Qu Yi and Dr. S. F. Yu for valuable discussions and careful reading of the manuscript. The authors also thank Dr. J. H. Teng and R. Tew for help in the measurement of the emission spectrum of the laser diodes.

[1] I. Kidoguchi, S. Kamiyama, M. Mannoh, Y. Ban, and K. Ohnaka, Appl. Phys. Lett. **62**, 2602 (1993).
[2] H. D. Summers and P. Blood, Electron. Lett. **29**, 1007 (1993).
[3] M. Ishikawa, Y. Ohba, H. Sugawara, M. Yamamoto, and T. Nakanishi, Appl. Phys. Lett. **48**, 207 (1986).
[4] P. M. Smowton and P. Blood, Appl. Phys. Lett. **67**, 1265 (1995).
[5] T. Kikkawa, H. Tanaka, and J. Komeno, J. Appl. Phys. **67**, 76 (1990).
[6] R. R. Saxena, J. E. Fouquet, V. M. Sard, and R. L. Moon, Appl. Phys. Lett. **53**, 304 (1988).
[7] M. E. Heimbuch, A. L. Holmes, Jr., M. P. Mack, S. P. DenBaars, L. A. Coldren, and J. E. Bowers, Electron. Lett. **29**, 340 (1993).
[8] W. J. Duncan, D. M. Baker, M. Harlow, A. English, A. L. Burness, and J. Haigh, Electron. Lett. **25**, 1603 (1989).
[9] J. C. Garcia, Ph. Maurel, and J. P. Hirtz, Electron. Lett. **29**, 432 (1993).
[10] K. Itaya, A. L. Holmes, Jr., S. Keller, S. G. Hummel, L. A. Coldren, and S. P. DenBaars, Jpn. J. Appl. Phys., Part 2 **34**, L1540 (1995).
[11] M. Mashita, H. Ishikawa, T. Izumiya, and Y. S. Hiraoka, Jpn. J. Appl. Phys., Part 1 **36**, 4230 (1997).
[12] J. R. Dong and S. J. Chua have also realized lasing from the same batch of wafers at room temperature (private communications).
[13] S. Yuan, Y. Kim, C. Jagadish, P. T. Burke, M. Gal, J. Zou, D. Q. Cai, D. J. H. Cockayne, and R. M. Cohen, Appl. Phys. Lett. **70**, 1269 (1997).
[14] S. Yuan, Y. Kim, C. Jagadish, P. T. Burke, M. Gal, M. C. Y. Chan, E. H. Li, and R. M. Cohen, J. Appl. Phys. **83**, 1305 (1998).
[15] C. T. H. F. Liedenbaum, A. Valster, A. L. G. J. Severens, and G. W. 't Hooft, Appl. Phys. Lett. **57**, 2698 (1990).
[16] P. Varshni, Physica (Utrecht) **34**, 149 (1967).
[17] I. Vurgaftman, J. R. Meyer, and L. R. Ram-Mohan, J. Appl. Phys. **89**, 5815 (2001).
[18] E. H. Li, Physica E (Amsterdam) **5**, 215 (1999).
[19] S. Iyer, S. Hegde, A. Abul-fadl, K. K. Bajaj, and W. Mitchel, Phys. Rev. B **47**, 1329 (1993).

[20] S. Z. Wang, S. F. Yoon, L. He, and X. C. Shen, J. Appl. Phys. **90**, 2314 (2001).
[21] P. Michler, A. Hangleiter, M. Moser, M. Geiger, and F. Scholz, Phys. Rev. B **46**, 7280 (1992).
[22] M. D. Dawson and G. Duggan, Phys. Rev. B **47**, 12598 (1993).
[23] K. L. Teo, J. S. Colton, and P. Y. Yu, Appl. Phys. Lett. **73**, 1697 (1998).
[24] M. L. Dotor, M. Recio, D. Golmayo, and F. Briones, J. Appl. Phys. **72**, 5861 (1992).
[25] D. S. Jiang, H. Jung, and K. Ploog, J. Appl. Phys. **64**, 1371 (1988).